Journal of Materials Chemistry B

Accepted Manuscript

ROYAL SOCIETY OF CHEMISTRY

www.rsc.org/materialsB

Journal Name

ARTICLE

A novel aminoclay-curcumin hybrid for enhanced chemotherapy

Suhang Wang,[a] Han Cao,[a] Yiming Zhong,[b] Yuhong Yang[c] and Zhengzhong Shao*[a]

Received 00th January 20xx,
Accepted 00th January 20xx

DOI: 10.1039/x0xx00000x

www.rsc.org/

Curcumin (Cur) has been demonstrated as an efficacious anti-tumor agent. However, its therapeutic applications are largely limited by its extremely low aqueous solubility, low stability and poor bioavailability. In this work, a simple one-pot synthesis was developed to fabricate a novel aminoclay-curcumin (AC-Cur) hybrid via the *in situ* loading of Cur over AC. The resultant hybrid was amenable to exfoliation and readily dispersable in aqueous media. Compared with free Cur, the AC-Cur hybrid displayed significantly enhanced solubility of Cur in both acid and neutral environments, as well as enhanced stability of Cur in both neutral and alkaline environments. More importantly, this hybrid achieved a much better therapeutic effect than free Cur against various tumor cell lines, which was mainly attributed to its significantly improved solubility, stability and cellular uptake. Our results suggest that such an AC-Cur hybrid with high bioavailability can potentially be applied in nanomedicine for the treatment of malignant tumours.

1. Introduction

Curcumin (Cur), a natural diphenolic compound derived from turmeric Curcuma longa, has been regarded as a promising anti-tumor agent because of its demonstrated effectiveness in inhibiting tumor cell survival and proliferation as well as in inducing apoptosis without promoting the development of side effects.[1-3] However, the clinical applications of Cur have been limited by its extremely low aqueous solubility, rapid systemic elimination, inadequate tissue absorption and degradation at neutral and alkaline pH conditions, which severely curtail its bioavailability.[1-6] In an attempt to overcome these limitations, a number of studies have been conducted, mainly focusing on the design of optimized delivery systems, including the employment of various drug carriers such as liposomes, polymeric nanoparticles or micelles, peptides, cyclodextrins, etc.[7-10]

Over the past decade, natural clays have attracted increasing attention since they have shown great potential in a wide range of applications in fields of catalysis,[11] biology,[12] medicine,[13] etc. For example, some functional clays were prepared by loading montmorillonite[14] and halloysite nanotubes,[15-17] which show poor dispersibility, with Cur to form nanocomposites. However, the dispersibility of such nanocomposites in water was undesirable. As is well acknowledged, many biological and catalytic applications necessitate the synthesis of functional clays that are water-solubilized and capable of interacting with desired molecules or substrates.[18,19] Therefore, those "water insoluble" nanocomposites are not desirable candidates to be applied in biological environment.

In comparison, a synthetic organic nanoclay, comprising 3-aminopropyl functionalized magnesium phyllosilicate (commonly referred to as *aminoclay*, AC), has shown promising prospects. It can be delaminated and stably dispersed in aqueous medium, because of the electrostatic repulsive forces between pendant quaternary ammonium groups.[20] The inherent properties of AC have been exploited for various applications, such as metal nanoparticle stabilizer,[21] drug delivery,[22] guest molecule encapsulation,[23] crosslinkers for organic polymers to form nanocomposite hydrogels,[24] etc. Although the biomedical application of AC is still at the exploratory stage, it has been regarded as applicable in developing drug carriers for controlled and targeted drug delivery with reduced risks to the environment and nontoxic to human beings.[25,26] Moreover, it has good potential to be developed into a drug delivery carrier to improve the bioavailability of poorly soluble drugs.[27,28] In previous studies, the poorly soluble drugs were mostly added in the exfoliated AC suspensions to produce drug-AC complexes via the electrostatic interactions. Those stepwise synthetic approaches were relatively complicated and the resultant drug-AC complexes were water insoluble and could only be used in an oral delivery system.

Though Cur has very low water solubility (11 ng/mL),[29] it can be easily dissolved in ethanol. On the other hand, AC can be prepared via a sol-gel process in ethanol at ambient conditions.[20] Based on these two considerations, a simple "one-

[a] State Key Laboratory of Molecular Engineering of Polymers, Department of Macromolecular Science, Laboratory of Advanced Materials, Fudan University, Shanghai, 200433, People's Republic of China. *E-mail: zzshao@fudan.edu.cn; Tel: +86 21 6564 2866

[b] Fuels and Energy Technology Institute & Department of Chemical Engineering, Curtin University, Perth, WA 6102, Australia.

[c] Research Center for Analysis and Measurement, Fudan University, Shanghai, 200433, People's Republic of China.

† Electronic supplementary information (ESI) available. See DOI: 10.1039/x0xx00000x

pot" synthesis was developed in this study to fabricate a dispersible AC-Cur hybrid which is amenable to followed exfoliation in aqueous conditions. The solubility and the stability of the AC-Cur hybrid nanoplates were examined; and the cytotoxicity of the hybrid was investigated, using three types of tumor cell lines, i.e. human cervical carcinoma (HeLa) cells, hepatocellular carcinoma (HepG2) cells and breast carcinoma (MDA-MB-231) cells. Compared with free Cur, the AC-Cur hybrid prepared via the one-step synthesis developed in this work exhibited enhanced solubility, stability and superior bioavailability of Cur.

2. Experimental Section

2.1 Materials.

3-aminopropyltriethosysilane (APTES) and Cur were purchased from Aladdin. Magnesium chloride hexahydrate ($MgCl_2 \cdot 6H_2O$) and ethanol were purchased from Sinopharm Chemical Reagent Co., Ltd, China. Phosphate buffered saline (PBS, 0.01 mol/L, pH 7.4) and 4', 6-diamidino-2-phenylindole (DAPI) were purchased from MesGen Biotechnology Co., Ltd. (China). Cell Counting Kit-8 (CCK-8) assay was purchased from Dojindo Laboratorise, Japan. Gibco fetal bovine serum (FBS), Dulbecco's modified Eagle's medium (DMEM) and minimum essential medium (MEM) were supplied by Invitrogen (Waltham, MA, USA). The other chemicals were all purchased and used as received without further purification if not specified.

2.2 Preparation and Characterization of the AC-Cur Hybrid.

The AC-Cur hybrid was prepared via a one-step synthesis which was developed based on a reported method for the preparation of AC.[25] Briefly, $MgCl_2 \cdot 6H_2O$ (0.84 g, 4.13 mmol) and Cur (10 mg) were dissolved in ethanol (20 g). APTES (1.3 mL, 5.85 mmol) was added dropwise with rapid stirring. After mixing for about 5 min, orange slurry was formed. To ensure sufficient equilibrium time for the formation of the AC-Cur hybrid, the reaction slurry was kept under stirring overnight. The precipitate was obtained via centrifugation, followed by washing with ethanol and vacuum drying. The Cur loading on AC was determined to be 4.25 μg/mg. For the exfoliation of the resulting AC-Cur hybrid, the bulk powder was dispersed in water under ultrasonication for 5 min.

Transmission electron microscope (TEM) analysis was performed with a FEI Tecnai G2 instrument at 200 kV. For sample preparation, diluted solution of the AC-Cur hybrid was directly dropped on a TEM grid and allowed to dry slowly at room temperature.

The particle size of the AC-Cur hybrid was measured at 25 °C with a Zetasizer Nano instrument (Malvern Inst. Ltd., UK) equipped with dynamic light scattering (DLS) (He−Ne laser, 633 nm wavelength). The concentration of the AC-Cur hybrid was 100 μg/mL and the total volume was 1 mL. The experiment was conducted in triplicates.

X-ray diffraction (XRD) data were recorded on an X' pert Pro with Cu Kα radiation, at 40 kV and 40 mA. The samples were scanned from 3^o to 70^o at a rate of 2^o/min.

2.3 Stability Analysis.

The stabilities of free Cur and the AC-Cur hybrid in the alkaline and the neutral environments were studied using Hitachi UV 2910 UV-vis spectrometer. A certain amount of free Cur was dissolved in a sodium hydroxide solution (pH 10) at the concentration of 4 μg/mL. The AC-Cur hybrid was dissolved in deionized water at the concentration of 6.5 μg/mL (pH 10). Afterwards, both solutions were incubated for different periods of time at room temperature in darkness. At the predetermined time points, 0.5 mL of each solution was sampled and analysed via a UV spectrometer. To examine the stability in the physiological condition, both solutions prepared following the above methods were separately added into the PBS (0.01 mol/L, pH 7.4). The pH values of the solutions were ensured to be around 7.4. The solutions were incubated at 37 °C in darkness for different periods of time; and then sampled and measured via the UV spectrometer.

2.4 *In Vitro* Release Kinetics.

The solutions of the exfoliated AC-Cur hybrid were placed in dialysis tubing (molecular weight cutoff (MWCO), 12-14 kDa) and immerged respectively into the PBS solutions (0.01 mol/L) at different pH values (i.e. 5.5, 6.5 and 7.4) at 37 °C in a constant temperature shaker for one week. At the predetermined time points, the released concentration of Cur in the dialysate solution was determined by the UV spectrometer. Fresh PBS was added to ensure that sink conditions were maintained unchanged throughout the experiment. It is worth noting that *in vitro* Cur release from the AC-Cur hybrid in the 0.01 mol/L PBS solution at pH 7.4 was also investigated by using dialysis tubing with a much lower MWCO (500-1000 Da). As shown in **Figure S1**, no significant difference was observed throughout the whole release period between the use of dialysis tubing with a 500-1000 Da MWCO and a 12-14 kDa MWCO. Therefore, what diffused across the membrane of dialysis tubing with a 12-14 kDa MWCO can be attributed to the free or released Cur, instead of the whole AC-Cur hybrid.

2.5 Cell Culture.

HeLa, HepG2 and MDA-MB-231 cells were purchased from the cell bank of Chinese Academy of Science (Shanghai, China). The HeLa, MDA-MB-231 cells were cultured in DMEM, and HepG2 cells was cultured in MEM, both supplemented with 10% FBS, 100 U/mL penicillin and 100 μg/mL streptomycin at 37 °C using a humidified 5% CO_2 incubator.

2.6 Colocalization by LSCM.

HeLa cells were seeded on a 35-mm glass bottom culture dish at 2×10^5 cells/well. At about 50% cell confluence, the media were removed and the cells were rinsed twice with serum-free

DMEM, and then replenished with 2 mL DMEM containing free Cur and the AC-Cur hybrid (2 μg Cur/well). After different incubation periods, the media were removed and the cells were washed three times with PBS. Afterwards, the cells were immobilized by 4% paraformaldehyde for 10 min, and stained with DAPI for 15 min. The media were removed and the cells were further washed several times with PBS, followed by refilling the wells with 2 mL PBS. Finally, the cells were imaged using laser scanning confocal microscope (LSCM, Olympus Fluoview FV 1000).

2.7 *In Vitro* Cytotoxicity Studies.

The cytotoxicity of free Cur and the AC-Cur hybrid against HeLa, HepG2 and MDA-MB-231 cells was determined by CCK-8 assay. The cells were seeded in 96-well plates (1×10^4 cells/well) with DMEM or MEM supplemented with 10% FBS and incubated at 37 °C with 5% CO_2 for 24 h. After removing the media, 200 μL of DMEM or MEM containing different concentrations of free Cur and the AC-Cur hybrid were added, followed by further incubation for different periods of time. Then, the culture media were replaced with fresh serum-free DMEM or MEM; and CCK-8 was added in darkness according to the protocol. The absorbance of the solution at 450 nm was tested using an Elx 800 instrument (Biotek, USA) after incubation for 2 h. The relative cell viability (%) was calculated as follows:

$$\text{Cell Viability (\%)} = \frac{[A]_{test}}{[A]_{control}} \times 100\%$$

Where $[A]_{test}$ is the absorbance of the test sample and $[A]_{control}$ is the absorbance of the control sample without any materials.

2.8 Data Analysis.

Differences between the means were analysed using one-way ANOVA analysis and Tukey's test. Differences between the group means were considered significant at $p < 0.05$ (*), $p < 0.01$ (**), and $p < 0.001$ (***); and NS, no significant difference, $p > 0.05$.

3. Results and Discussion

3.1 Preparation and Characterization.

The AC-Cur hybrid was prepared via a simple one-step mixing method for the purpose of enhancing the solubility and bioavailability of entrapped Cur in aqueous solutions. The *in situ* formation of the AC-Cur hybrid is illustrated in **Schematic 1a**. APTES was added dropwise into the ethanol solution containing

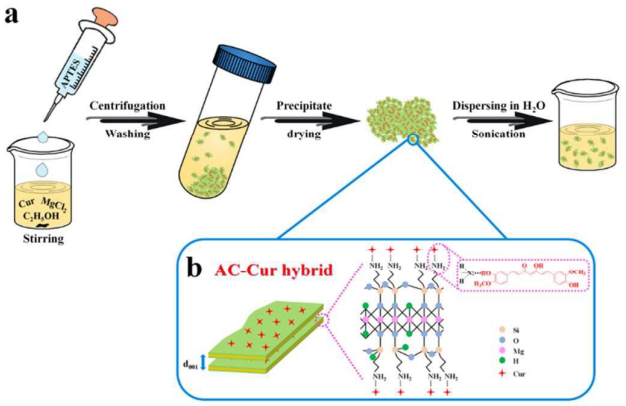

Schematic 1. (a) Preparation of the AC-Cur hybrid. (b) Two dimensional structural representation of aminopropyl-functionalized magnesium phyllosilicate and the interaction with Cur.

$MgCl_2 \cdot 6H_2O$ and Cur with rapid stirring, and the AC-Cur hybrid was readily produced. In this sol-gel process, APTES and $MgCl_2 \cdot 6H_2O$ are employed as the precursors for the formation of the aminopropyl-functionalized silicate network which involves the silicon-magnesium binary oxides. Binary oxides have attracted much attention because of their improved properties compared to the individual oxides.[30] In particular, silica-magnesia mixed oxides with tunable acid-base properties have shown controlled chemical affinity toward substances,[31,32] which is a favorable characteristic for applications in drug delivery.

The XRD patterns of free Cur, AC and the AC-Cur hybrid were shown in **Figure 1a**. The characteristic diffraction peak (060) was observed around $2\theta = 59^o$, corresponding to the 2:1 trioctahedral smectite structure which consists of a central brucite sheet of octahedrally coordinated MgO/OH chains overlaid on both sides with an aminopropyl-functionalized silicate network for the AC and AC-Cur hybrid (**Schematic 1b**),[33,34,35] suggested that the structural framework of AC was retained during the interaction with Cur (the drug molecule). Meanwhile, for the d_{001} interlamellar spacing, no significant difference was observed between AC and the AC-Cur hybrid, indicating the interaction between Cur and the surface of the AC lamellae rather than the intercalation of the drug molecules into the interlayer space of AC.[28] On the other hand, according to the XRD pattern of free Cur, it has high crystallinity in nature, with a most distinctive peak at 17.3°. When Cur was loaded on AC (i.e. in the case of the AC-Cur hybrid), notably,

no sharp, well defined peak was observed, which suggested that the interaction between Cur and AC in the molecular level prevented the crystallization of Cur. The differential scanning calorimetry (DSC) analysis was conducted to further investigate the physical state of Cur in the hybrid. As shown in **Figure S2**, the endothermic peak (melting point) of Cur was observed at around 176 °C. In comparison, for the AC-Cur hybrid, such an endothermic peak was not observed.

The TEM image of the AC-Cur hybrid was shown in **Figure 1b**. According to the TEM image, the average size of the resulting delaminated nanoplates with spherical geometry was determined to be 143 ± 14 nm. Considering that particle size is an important parameter for the study of cellular uptake, the particle size distribution of the AC-Cur hybrid in the aqueous medium was further investigated by DLS. According to the DLS result (inset in **Figure 1b**), the average particle size of the AC-Cur hybrid was determined to be 139 ± 17 nm, which was consistent with the TEM result, and was considered to be beneficial for the cellular and tissue uptake.[36]

3.2 Solubility.

As is commonly acknowledged, free Cur is poorly soluble in aqueous media at acidic and neutral pH. Although it is easily dissolved in alkaline conditions, Cur would precipitate as micro-flakes when the solution was gradually adjusted to neutral and even further to acidity (**Figure 1c, left**, highlighted by the blue circle). In contrast, the prepared AC-Cur hybrid not only displayed a clear, well dispersed formulation with the natural colour of Cur in the alkaline environment (pH 10, same pH value as that of the exfoliated AC solution), but also remained soluble when the aqueous alkaline solution was acidified to pH 7.4 or to pH 1 (**Figure 1c, right**). It is worth noting that a small amount of Cur could dissolve in the exfoliated AC solution because of the initial alkaline environment of the AC solution. However, such dissolved Cur would still precipitate when the solution was acidified. In this regard, it can be further speculated that for the AC-Cur hybrid prepared via the sol-gel method established in this study, Cur was loaded on AC via some intermolecular interactions rather than simple adsorption. Such interactions contribution to the stabilization of the AC-Cur hybrid dispersion against precipitation over a wide range of pH in the aqueous environment. Podaralla et al. synthesized a novel biodegradable micelle by conjugating methoxypoly(ethylene glycol) to zein; and the micelle significantly enhanced the aqueous solubility of Cur by 1000-2000-fold.[29] In the formulation developed in this work, the solubility of Cur in the AC-Cur hybrid was 15.6 ± 0.5 μg/mL in the acidic environment (pH 1) and 49.7 ± 0.9 μg/mL in the neutral environment (pH 7.4), which showed a 4500-fold increase compared with that of free Cur (11 ng/mL).

3.3 Stability.

Besides its low solubility in water, the remarkable instability of the Cur molecule in the alkaline and the physiological pH conditions is another major limiting factor for its bioapplication.[5] In order to investigate the stability of Cur in the AC-Cur hybrid

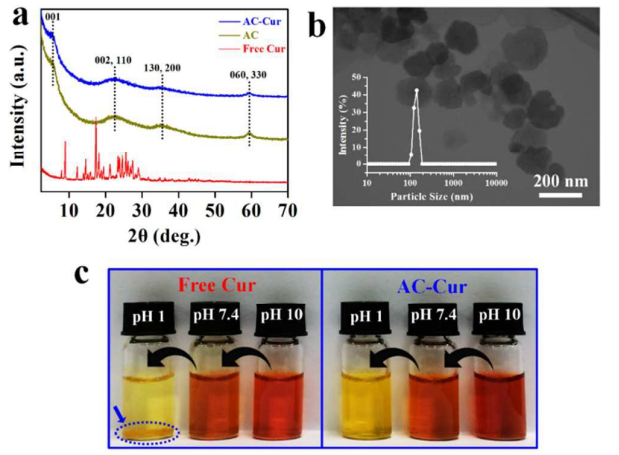

Figure 1. Characterization of the AC-Cur hybrid. (a) XRD diffraction patterns of free Cur, AC and the AC-Cur hybrid. (b) TEM image of the AC-Cur hybrid. The inset showed the size distribution of the AC-Cur hybrid measured by DLS. (c) Left: free Cur was dissolved in 0.1 mol/L sodium hydroxide solution with the initial pH value of 10. Right: AC-Cur hybrid was dissolved in deionized water (the initial pH value of the solution was 10, attributed to the involving of AC). The weight concentration of Cur in both samples was 10 μg/mL. Hydrochloric acid (0.1 mol/L) was used to acidify the solution (pH changed from 10 to 7.4 and to 1, as indicated by the black arrows).

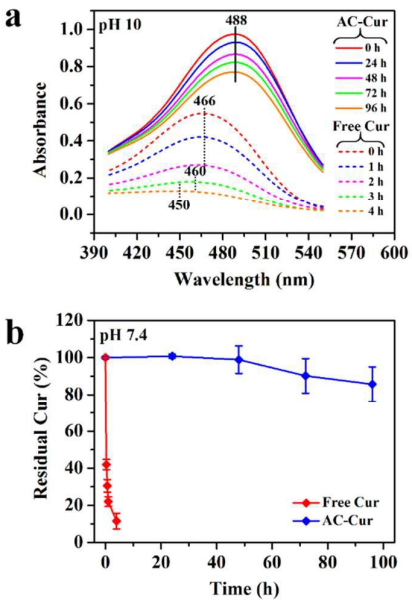

Figure 2. Cur Stability examined via UV-Vis spectroscopy. (a) Absorption spectra of free Cur and the AC-Cur hybrid at different incubation times in the same pH condition (pH 10) at room temperature in darkness. (b) The changes of the absorption intensities as a function of incubation time in 0.01 mol/L PBS (pH 7.4) at 37 °C in darkness.

fabricated in this study, the UV-Vis absorption spectra of free Cur and the AC-Cur hybrid in the alkaline environment incubated for different periods of time were measured. As shown in **Figure 2a** and **Figure S3**, the absorption band of free Cur peaked at 466 nm. As the incubation time increased, blue-shift of the maximum absorption wavelength was observed with a decrease in intensity. This indicated the dramatic degradation of free Cur in the alkaline condition. The three main degraded products of Cur were identified as vanillin, ferulic acid and feruloylmethane (**Figure S4a**).[37] By comparison, Cur in the AC-Cur hybrid was found to be much more stable than the one in its free form (**Figure 2a**, **S3** and **S4b**). According to **Figure 2a**, the maximum absorption shifted to a longer wavelength of around 488 nm at pH 10, which was most likely to be attributed to the formation of the strong hydrogen bonds between the hydroxyl groups of Cur and the amino groups of AC (**Schematic 1b**).[3,38,39]

The stability/biodegradability of Cur in the physiological condition, which is critically important for its bioapplication,[4,5] was further examined. As shown in **Figure 2b**, free Cur degraded rapidly in the PBS solution (0.01 mol/L, pH 7.4), with only 12% of Cur remaining after 4 h of incubation. By comparison, Cur in the AC-Cur hybrid was remarkably stable under the same condition, with more than 85% of Cur remaining after 4 days of incubation. According to this result, the hybrid developed in this study shows superior stability over many reported formulations. For example, Manju et al. reported that by conjugation with hyaluronic acid, 90% of Cur remained after 8 h of incubation in an aqueous solution at pH 7.4.[40] However, 90% of Cur in the AC-Cur hybrid remained after 72 h of incubation under the same condition. These results suggested that the formulation developed in this study favours the bioapplication of Cur in terms of the significantly improved solubility and stability of Cur.

3.4 *In Vitro* Release Kinetics.

To the best of our knowledge, the extracellular environment of tumour is more acidic (pH 6.5) than that of blood and normal tissues (pH 7.4); and the pH values of endosome and lysosome are even as low as 5.0-5.5.[41] In this study, time-dependent cumulative release of Cur from the AC-Cur hybrid in different pH conditions (i.e. pH 5.5, 6.5, 7.4) was investigated. As shown in **Figure 3**, a rapid release of about 18% of Cur loaded in the AC-Cur hybrid was observed for the first day, followed by a sustained release until about 40% of Cur liberated within 7 days. No significant difference was observed between the Cur-release curves of the AC-Cur hybrid in different pH conditions throughout the whole release period. It is most likely that the rapid release of Cur in the first day was attributed to the Cur molecules directly absorbed in AC; and the sustained release mainly resulted from Cur that strongly interacted with AC. Therefore, this AC-Cur hybrid can potentially be used as a controlled-release formulation.

3.5 Cellular Uptake.

Due to the photochemical properties of Cur, the intracellular uptake of free Cur and of the AC-Cur hybrid can be easily examined by fluorescent imaging. The HeLa cells with different periods of post incubation time were imaged by LSCM. As shown in **Figure 4**, free Cur was quickly transported into the cells by passive diffusion. However, at 6 h post-incubation, weakened fluorescence was observed for the HeLa cells treated with free Cur, compared with that observed at 2 h post-incubation. This mainly resulted from the instability of free Cur in both the extracellular and the intracellular environments. In comparison, intensified fluorescence was observed in the cells treated by the AC-Cur hybrid; and was further enhanced with the increase of incubation time. It was suggested that the AC-Cur hybrid could be internalized by and accumulated in the cells. Furthermore, the cellular uptake efficiency of free Cur and the

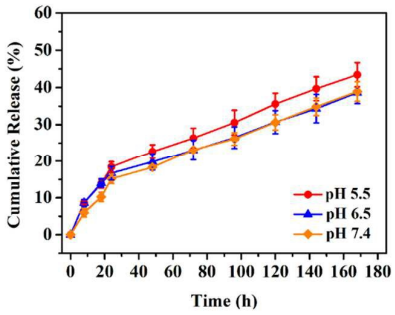

Figure 3. Time-dependent cumulative release of Cur from the AC-Cur hybrid in different pH conditions.

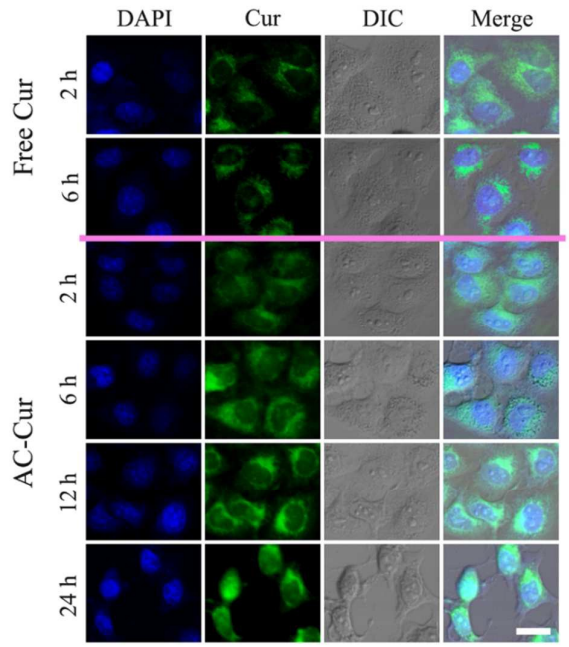

Figure 4. LSCM images of free Cur and the AC-Cur hybrid in HeLa cells at 37 °C under an atmosphere of 5% CO_2. The cells were imaged at different time post-incubation. Blue: DAPI-labeled cell nucleus; green: Cur (1 μg/mL). Scale bar: 20 μm.

AC-Cur hybrid at the first 2 h of incubation was evaluated by flow cytometry (FCM). As can be seen in **Figure S5**, the mean fluorescence intensity of the cells treated by free Cur decreased over time. On the contrary, that of the cells treated by the AC-Cur hybrid increased over the two hours, with values consistently higher than that of its counterpart. Considering that Cur in the AC-Cur hybrid is more stable than free Cur and the AC-Cur hybrid could be efficiently internalized by the cells, the bioactive Cur molecules could be slowly released from the AC-Cur hybrid for a relatively long period of time.

3.6 *In Vitro* Cytotoxicity Studies.

Although the cellular uptake investigation presented a better cell uptake of the active Cur in the AC-Cur hybrid than that of free Cur, the analysis of cell cytotoxicity is equally important for the evaluation of the pharmacological activity of the drug. Therefore, the *in vitro* cell cytotoxicity of both free Cur and the AC-Cur hybrid against various tumor cell lines, i.e. HeLa cells, HepG2 cells and MDA-MB-231 cells were determined by the CCK-8 assay.

As shown in **Figure 5a**, **b** and **c**, both free Cur and the AC-Cur hybrid showed dose dependent anti-tumor effects on the HeLa cells with different periods of post incubation time. However, based on the IC_{50} (concentration of drug required to kill 50% of cells) values (**Figure 5d**), the AC-Cur hybrid displayed much better anti-tumor effect compared with free Cur. For example, the IC_{50} values of the AC-Cur hybrid and free Cur

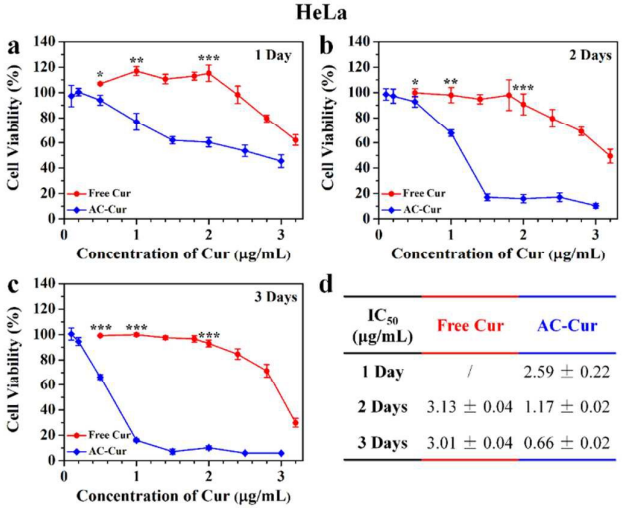

Figure 5. HeLa cell viability after the treatment of free Cur and the AC-Cur hybrid for (a) 1 day; (b) 2 days; and (c) 3 days (n=4). Cell viability of control (untreated HeLa cells): 100%. (d) Comparison of the IC_{50} (μg/mL) values. Data are expressed as mean ± SD (n=4).

were 2.59 ± 0.22 vs >3.20, 1.17 ± 0.02 vs 3.13 ± 0.04 and 0.66 ± 0.02 vs 3.01 ± 0.04 μg/mL after incubated for 1, 2 and 3 days, respectively. Similar superior anti-tumor effects of the AC-Cur hybrid were also observed on the HepG2 cells (**Figure S6**) and the MDA-MB-231 cells (**Figure S7**). In addition, HeLa cells, HepG2 cells or MDA-MB-231 cells were individually co-cultured with Cur-free AC at concentrations ranging from 0.01 to 1.0 mg/mL for 3 days. None of these tumor cells was influenced by the addition of AC (**Figure S8**), which indicated

that the cell cytotoxicity of the drug-loaded hybrid mainly resulted from the Cur component rather than the carrier, AC.

According to this result, the hybrid developed in this study shows superior anti-tumor effects over many reported formulations. For example, Mohanty et al. have developed a Cur-loaded nanoparticulate delivery system by the use of glycerol monooleate and pluronic F-127. Nanoparticulate Cur is 1.52, 3.4, 1.23, 2.05, 1.87 and 2.48 times (IC_{50} values) more effective than free Cur as observed in PANC-1, MIA PaCa-2, K562, MCF-7, HCT-116 and A549 cell line respectively.[42] In this study, the low IC_{50} values of the AC-Cur hybrid are most likely to be attributed to the strong interactions between AC and Cur. As is well known, the anti-tumor effect of a drug is very well correlated with the duration of its intercellular retention and stability.[43] Compared to free Cur, Cur in the AC-Cur hybrid shows superior stability and sustained release in the physiological condition, resulting in the significant improvement of its anti-proliferative effect, especially for a relative long term.

4. Conclusions

In this study, we successfully developed a one-step sol-gel method to fabricate a novel AC-Cur hybrid by the *in situ* loading of Cur over AC, as supposed there was strong interaction between two components. Such AC-Cur hybrid was readily dispersed in aqueous media and significantly enhanced the aqueous solubility of Cur by 4500-fold. Moreover, the AC-Cur hybrid showed largely enhanced stability of Cur in both neutral and alkaline conditions. Consistently, compared with free Cur, the AC-Cur hybrid showed greater inhibitory effect on the growth of various tumor cell lines due to the protection of AC to those loaded bioactive Cur molecules. Therefore, the AC-Cur hybrid presented the potential to be a nanomedicine for chemotherapy in the future, as it was beneficial for the improvement of sustained bioavailability of Cur.

Acknowledgements

This work was supported by National Natural Science Foundation of China (No. 21574024, 21374020). We thank Prof. Xin Chen, Dr. Jinrong Yao and Xia Zhang at Fudan University for their valuable discussions.

Notes and references

1 M. Salem, S. Rohani and E. R. Gillies, *RSC Adv.*, 2014, **4**, 10815-10829.
2 R. Wilken, M. S. Veena, M. B. Wang and E. S. Srivatsan, *Mol. Cancer*, 2011, **10**, 12.
3 M. Heger, R. F. van Golen, M. Broekgaarden and M. C. Michel, *Pharmacol. Rev.*, 2014, **66**, 222-307.
4 P. Anand, A. B. Kunnumakkara, R. A. Newman and B. B. Aggarwal, *Mol. Pharmaceutics*, 2007, **4**, 807-818.
5 Y. J. Wang, M. H. Pan, A. L. Cheng, L. I. Lin, Y. S. Ho, C. Y. Hsieh and J. K. Lin, *J. Pharm. Biomed. Anal.*, 1997, **15**, 1867-1876.
6 S. Prasad, A. K. Tyagi and B. B. Aggarwal, *Cancer Res. and Treat.*, 2014, **46**, 2-18.
7 O. Naksuriya, S. Okonogi, R. M. Schiffelers and W. E. Hennink, *Biomaterials*, 2014, **35**, 3365-3383.
8 M. M. Yallapu, M. Jaggi and S. C. Chauhan, *Drug Discovery Today*, 2012, **17**, 71-80.
9 W. H. Lee, C. Y. Loo, P. M. Young, D. Traini, R. S. Mason and R. Rohanizadeh, *Expert Opin. Drug Delivery*, 2014, **11**, 1183-1201.
10 M. Sun, X. Su, B. Ding, X. He, X. Liu, A. Yu, H. Lou and G. Zhai, *Nanomedicine*, 2012, **7**, 1085-1100.
11 S. Miao, Z. Liu, B. Han, J. Huang, Z. Sun, J. Zhang and T. Jiang, *Angew. Chem., Int. Ed.*, 2006, **45**, 266-269.
12 M. Liu, Y. Shen, P. Ao, L. Dai, Z. Liu and C. Zhou, *RSC Adv.*, 2014, **4**, 23540-23553.
13 M. Liu, C. Wu, Y. Jiao, S. Xiong and C. Zhou, *J. Mater. Chem. B*, 2013, **1**, 2078-2089.
14 N. Madusanka, K. M. N. de Silva and G. Amaratunga, *Carbohydr. Polym.*, 2015, **134**, 695-699.
15 M. Massaro, S. Riela, P. Lo Meo, R. Noto, G. Cavallaro, S. Milioto and G. Lazzara, *J. Mater. Chem. B*, 2014, **2**, 7732-7738.
16 S. Riela, M. Massaro, C. G. Colletti, A. Bommarito, C. Giordano, S. Milioto, R. Noto, P. Poma and G. Lazzara, *Int. J. Pharm*, 2014, **475**, 613-623.
17 G. Cavallaro, G. Lazzara, M. Massaro, S. Milioto, R. Noto, F. Parisi and S. Riela, *J. Phys. Chem. C*, 2015, **119**, 8944-8951.
18 A. C. Balazs, T. Emrick and T. P. Russell, *Science*, 2006, **314**, 1107-1110.
19 I. K. Tonlé, T. Diaco, E. Ngameni and C. Detellier, *Chem. Mater.*, 2007, **19**, 6629-6636.
20 K. K. R. Datta, A. Achari and M. Eswaramoorthy, *J. Mater. Chem. A*, 2013, **1**, 6707-6718.
21 K. K. R. Datta, C. Kulkarni and M. Eswaramoorthy, *Chem. Commun.*, 2010, **46**, 616-618.
22 P. Chaturbedy, D. Jagadeesan and M. Eswaramoorthy, *ACS Nano*, 2010, **4**, 5921-5929.
23 A. J. Patil and S. Mann, *J. Mater. Chem.*, 2008, **18**, 4605-4615.
24 J. E. Martin, A. J. Patil, M. F. Butler and S. Mann, *Adv. Funct. Mater.*, 2011, **21**, 674-681.
25 H. K. Han, Y. C. Lee, M. Y. Lee, A. J. Patil and H. J. Shin, *ACS Appl. Mater. Interfaces*, 2011, **3**, 2564-2572.
26 L. Yang, Y. C. Lee, M. I. Kim, H. G. Park, Y. S. Huh, Y. Shao and H. K. Han, *J. Mater. Chem. B*, 2014, **2**, 7567-7574.
27 L. Yang, S. K. Choi, H. J. Shin and H. K. Han, *Int. J. Nanomed.*, 2013, **8**, 4147-4155.
28 L. Yang, Y. Shao and H. K. Han, *Int. J. Pharm.*, 2014, **471**, 258-263.
29 S. Podaralla, R. Averineni, M. Alqahtani and O. Perumal, *Mol. Pharmaceutics*, 2012, **9**, 2778-2786.
30 R. Brambilla, J. Poisson, C. Radtke, M. S. L. Miranda, M. B. Cardoso, I. S. Butler and J. H. Z. dos Santos, *J. Sol-Gel Sci. Technol.*, 2011, **59**, 135-144.

31 T. López, R. Gomez, M. E. Llanos and E. López-Salinas, *Mater. Lett.*, 1999, **38**, 283-288.
32 K. Yamamoto, *Appl. Catal., A*, 2009, **368**, 65-70.
33 S. L. Burkett, A. Press and S. Mann, *Chem. Mater.*, 1997, **9**, 1071-1073.
34 N. T. Whilton, S. L. Burkett and S. Mann, *J. Mater. Chem.*, 1998, **8**, 1927-1932.
35 A. Achari, K. K. R. Datta, M. De, V. P. Dravid and M. Eswaramoorthy, *Nanoscale*, 2013, **5**, 5316-5320.
36 C. He, Y. Hu, L. Yin, C. Tang and C. Yin, *Biomaterials*, 2010, **31**, 3657-3666.
37 L. Shen and H. F. Ji, *Trends Mol. Med.*, 2012, **18**, 138-144.
38 F. Y. Wu, M. Z. Sun, Y. L. Xiang, Y. M. Wu and D. Tong, *J. Lumin.*, 2010, **130**, 304-308.
39 F. Zsila, Z. Bikádi and M. Simonyi, *Tetrahedron: Asymmetry*, 2003, **14**, 2433-2444.
40 S. Manju and K. Sreenivasan, *J. Colloid Interface Sci.*, 2011, **359**, 318-325.
41 E. S. Lee, Z. Gao and Y. H. Bae, *J. Controlled Release*, 2008, **132**, 164-170.
42 C. Mohanty and S. K. Sahoo, *Biomaterials*, 2010, **31**, 6597-6611.
43 Z. Ma, A. Haddadi, O. Molavi, A. Lavasanifar, R. Lai and J. Samuel, *J. Biomed. Mater. Res., Part A*, 2008, **86A**, 300-310.

Graphic for the Table of Contents